

Secure Rate Splitting in STAR-RIS Assisted Downlink MISO Systems

Hamid Reza Hashempour, Gilberto Berardinelli

Department of Electronic Systems, Aalborg University, Denmark

E-mail: {hrh, gb}@es.aau.dk

Abstract—This paper explores a secure downlink multiple-input single-output (MISO) system using simultaneously transmitting and reflecting reconfigurable intelligent surface (STAR-RIS) aided rate splitting multiple access (RSMA), where a base station transmits confidential signals to users, combating eavesdroppers in both transmission and reflection spaces of the RIS. Assuming known channel state information (CSI) at the base station, the RSMA strategy involves splitting user messages into common and private parts, aiming to maximize the sum secrecy rate under power and beamforming constraints. We address the non-convex optimization challenge through alternating optimization and the sequential convex approximation (SCA) method, focusing on both active and passive beamforming. Our simulations highlight notable enhancements in secrecy rate and spectral efficiency via STAR-RIS, underscoring the effectiveness of our algorithms. Furthermore, our approach outperforms the non-orthogonal multiple access (NOMA) technique.

Index Terms—Rate-Splitting, reconfigurable intelligent surfaces, simultaneous transmission and reflection, physical layer security.

I. INTRODUCTION

To address the need for faster data speeds and enhanced security in future 6G wireless networks, Reconfigurable Intelligent Surfaces (RIS) have emerged as pivotal. Comprised of affordable, adaptable components, RIS control incoming signals in novel ways, revolutionizing communication methods [1]. A significant breakthrough is Simultaneously Transmitting and Reflecting RIS (STAR-RIS), surpassing traditional RIS capabilities by enabling both signal reflection and transmission, ensuring comprehensive spatial coverage [2]. This dual functionality also bolsters secure communications, offering flexible countermeasures against eavesdropping attempts. Robustness against eavesdropping is crucial, particularly for use cases supporting critical communications like those in in-X subnetworks [3].

Within the framework of technological progress, Rate Splitting Multiple Access (RSMA) stands out for its capacity to boost spectral efficiency and fairness in multi-user communications, while also enhancing physical layer security (PLS) [4]. By dividing messages into common and private segments, RSMA offers a flexible and interference-resistant approach, outperforming traditional multiple access techniques [5]. The integration of STAR-RIS with RSMA, therefore, presents a compelling approach to bolstering both the efficiency and security of wireless networks. This synergy promises to exploit the full spatial coverage of STAR-RIS, while leveraging the flexibility of RSMA to maximize the sum secrecy rate

(SSR)—a critical metric in secure communications—under the constraints of known channel state information (CSI) at the Base Station (BS) and the presence of potential eavesdroppers.

Despite extensive research on RIS for network enhancement and security, the study of STAR-RIS within RSMA-based systems is relatively unexplored. While previous research has focused on STAR-RIS for secure communications, its integration with RSMA and effects on system performance and security are less understood. Our work introduces a new framework for MISO STAR-RIS-aided RSMA systems, enhancing SSR through beamforming optimization and filling a research void [6], [7]. While [6] investigates rate splitting in STAR-RIS without considering PLS, [7] adds PLS but ignores the BS-user direct link.

In this study, we consider both security and the direct link between BS and users. We introduce an innovative secure communication scheme that harnesses the dual capabilities of STAR-RIS in a RSMA setting, demonstrating its superiority over traditional access methods in mitigating eavesdropping risks. Furthermore, we propose a sophisticated optimization model that addresses the non-convex nature of the beamforming design problem, employing alternating optimization and the Sequential Convex Approximation (SCA) method to achieve efficient and practical solutions. Our extensive simulations confirm the effectiveness of our proposed strategies, demonstrating marked improvements in secrecy rate and network performance with an increasing number of STAR-RIS elements. Our method demonstrates superiority compared to both the non-orthogonal multiple access (NOMA) approach and STAR-RIS-RSMA with direct link blockage, which serve as baseline methods.

The remainder of the paper is organized as follows: Section II presents the system model of our approach. Section III elaborates on the proposed method for maximizing the SSR, including the optimization of active and passive beamforming. In Section IV, we provide a comprehensive evaluation of our approach through simulation results. Finally, Section V concludes the paper.

II. SYSTEM MODEL AND PRELIMINARIES

A. Model of STAR-RIS

This work utilizes an Energy Splitting (ES) model for STAR-RIS, enabling simultaneous signal transmission and reflection [2]. For the m -th RIS element, the incident signal s_m , where $m \in \mathbb{M} \triangleq \{1, 2, \dots, M\}$ and M is the number

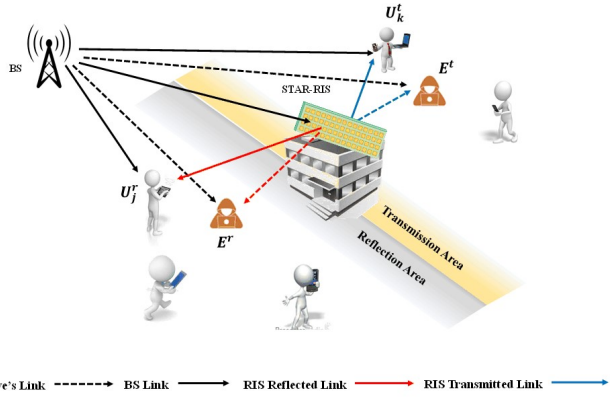


Fig. 1: Illustration of signal propagation in the STAR-RIS and the system model.

of RIS elements, is either transmitted $(\sqrt{\beta_m^t} e^{j\theta_m^t}) s_m$ or reflected $(\sqrt{\beta_m^r} e^{j\theta_m^r}) s_m$, with amplitude and phase shift coefficients $\{\sqrt{\beta_m^t}, \sqrt{\beta_m^r}\}$ and $\{\theta_m^t, \theta_m^r\}$, respectively. These are subject to energy conservation $\beta_m^t + \beta_m^r = 1, \forall m \in \mathbb{M}$, while $\{\theta_m^t, \theta_m^r\}$ are independently adjustable. We also denote the transmission/reflection beamforming vector as $\mathbf{u}_p = [\sqrt{\beta_1^p} e^{j\theta_1^p}, \sqrt{\beta_2^p} e^{j\theta_2^p}, \dots, \sqrt{\beta_M^p} e^{j\theta_M^p}]$ where $p = t$ for transmission and $p = r$ for reflection. The corresponding diagonal beamforming matrix of the STAR-RIS for transmission/reflection is given by $\Theta_p = \text{diag}(\mathbf{u}_p)$. The constraints for transmission and reflection coefficients are formalized as:

$$\mathbb{R}_\beta = \{\beta_m^t, \beta_m^r \mid \beta_m^t, \beta_m^r \in [0, 1]; \beta_m^t + \beta_m^r = 1\}, \quad (1)$$

$$\mathbb{R}_\theta = \{\theta_m^t, \theta_m^r \mid \theta_m^t, \theta_m^r \in [0, 2\pi)\}. \quad (2)$$

B. System Description

The system considers downlink transmission in a STAR-RIS assisted network with the BS having N_T transmit antennas and the STAR-RIS consisting of M elements. Users are categorized into transmission space users U_k^t and reflection space users U_j^r , with K/\mathcal{K} and J/\mathcal{J} being the total number/set of users in each category, respectively. Thus, the total number and set of users in the network are denoted by $N = K + J$ and $\mathcal{N} = \{\mathcal{K}, \mathcal{J}\}$, respectively.

Fig. 1 illustrates the system's communication paths, including direct links between the BS and single-antenna users, and RIS-mediated links. It also assumes the presence of eavesdroppers, E^t in the transmission space and E^r in the reflection space, wiretapping the channel. The channel from the BS to user U_n^p , with $p \in \{t, r\}$ and for all $n \in \mathcal{N}$, is represented by $\mathbf{h}_{p,n} = (\mathbf{g}_{b,n}^p)^H + \mathbf{g}_{p,n}^H \Theta_p \mathbf{H}$, where $\mathbf{g}_{b,n}^p \in \mathbb{C}^{N_T \times 1}$, and $\mathbf{H} \in \mathbb{C}^{M \times N_T}$ represent the channel vector from the BS to U_n^p and the channel matrix from the BS to the RIS, respectively. $\mathbf{g}_{p,n} \in \mathbb{C}^{M \times 1}$ is the channel vector from the RIS to U_n^p . The CSI of the U_k^t and U_j^r is assumed to be known at the transmitter.

C. Signal Model

As assumed in the literature on RSMA [8], the BS divides the message W_n of n th user into a common part $W_{c,n}$ and a private part $W_{p,n}, \forall n \in \mathcal{N}$. The common stream s_c is achieved by jointly encoding the common parts of all

users $\{W_{c,1}, \dots, W_{c,N}\}$. The private streams $\{s_1^t, \dots, s_K^t\}$ are obtained by independently encoding the private parts of the users. Therefore, the total transmit signal is given by

$$\mathbf{x} = \mathbf{x}^t + \mathbf{x}^r = \mathbf{p}_c s_c + \sum_{k \in \mathcal{K}} \mathbf{p}_k s_k^t + \sum_{j \in \mathcal{J}} \mathbf{p}_{K+j} s_j^r, \quad (3)$$

where \mathbf{p}_c , and $\mathbf{p}_n \in \mathbb{C}^{N_T \times 1}$ are the precoders for the common, and the private signals of users in the transmission and reflection spaces, respectively. We denote $\mathbf{P} = [\mathbf{p}_c, \mathbf{p}_1, \dots, \mathbf{p}_K, \mathbf{p}_{K+1}, \dots, \mathbf{p}_{K+J}]$ as the information precoder matrix. The set of $\mathbf{s} = [s_c, s_1^t, \dots, s_K^t, s_1^r, \dots, s_J^r]^T \in \mathbb{C}^{(K+J+1) \times 1}$ represents the user streams. Under the assumption that $\mathbb{E}\{\mathbf{s}\mathbf{s}^H\} = \mathbf{I}$, the transmit power constraint is $\text{Tr}(\mathbf{P}\mathbf{P}^H) \leq P_t$, where P_t is the total available transmit power. The signals received at U_n^p is given by

$$y_n = \mathbf{h}_{p,n} \mathbf{x} + z_n, \quad p \in \{t, r\}, \quad \forall n \in \mathcal{N}, \quad (4)$$

where the term z_n represents additive Gaussian noise with zero mean and unit variance received at U_n^p . According to the standard RSMA decoding order [8], before decoding the intended private stream, the common stream is decoded by each user while treating the private streams as interference. Hence, the Signal-to-Interference-plus-Noise Ratio (SINR) for decoding common stream s_c at U_n^p is

$$\gamma_{c,n}^p = \frac{|\mathbf{h}_{p,n} \mathbf{p}_c|^2}{\sum_{n' \in \mathcal{N}} |\mathbf{h}_{p,n} \mathbf{p}_{n'}|^2 + 1}, \quad \forall n \in \mathcal{N}, \quad p \in \{t, r\}. \quad (5)$$

The contribution of s_c is removed from y_n after decoding. Then, the intended private stream s_n^p of U_n^p can be decoded by treating the interference from other users as noise. The SINR for decoding the private stream s_n^p at U_n^p is:

$$\gamma_n^p = \frac{|\mathbf{h}_{p,n} \mathbf{p}_n|^2}{\sum_{n' \in \mathcal{N}, n' \neq n} |\mathbf{h}_{p,n} \mathbf{p}_{n'}|^2 + 1}, \quad \forall n \in \mathcal{N}, \quad p \in \{t, r\}. \quad (6)$$

The achievable information rates of s_c , s_k^t , and s_j^r at U_k^t and U_j^r can be respectively written as:

$$R_{c,n}^p = \log_2(1 + \gamma_{c,n}^p), \quad \forall n \in \mathcal{N}, \quad p \in \{t, r\}, \quad (7)$$

$$R_n^p = \log_2(1 + \gamma_n^p), \quad \forall n \in \mathcal{N}, \quad p \in \{t, r\}. \quad (8)$$

Since it is required that all users decode the common stream, the achievable rate of s_c can not exceed the minimum achievable rate of all users, i.e., $R_c = \min\{R_{c,1}^p, \dots, R_{c,N}^p\}$, $p \in \{t, r\}$. Assume that the common rate R_c is shared by all N users, and let C_n denote the portion of R_c transmitting $W_{c,n}$, so that we have $C_n = \alpha_n R_c$ where $\sum_{n=1}^N \alpha_n = 1$. Therefore, the overall achievable rate of U_k^t and U_j^r are given by $R_{k,tot} = C_k + R_k^t$ and $R_{j,tot} = C_j + R_j^r$, respectively, which both include common and private rates $W_{c,n}$ and $W_{p,n}$.

We assume that the two eavesdroppers E^t and E^r are in the transmission and reflection spaces, respectively, and can wiretap the user channels and that know the precoder matrix \mathbf{P} . Thus, the SINR for decoding the common stream s_c and the private stream $s_n^p, p \in \{t, r\}$ are:

$$\gamma_{c,e}^p = \frac{|\mathbf{h}_{p,e} \mathbf{p}_c|^2}{\sum_{n \in \mathcal{N}} |\mathbf{h}_{p,e} \mathbf{p}_n|^2 + 1}, \quad (9)$$

$$\gamma_{e,n}^p = \frac{|\mathbf{h}_{p,e}\mathbf{p}_n|^2}{|\mathbf{h}_{p,e}\mathbf{p}_c|^2 + \sum_{n' \in \mathcal{N}, n' \neq n} |\mathbf{h}_{p,e}\mathbf{p}_{n'}|^2 + 1}, \forall n \in \mathcal{N}. \quad (10)$$

It is worth noting that $\mathbf{h}_{p,e}$ is the combined channels of E^p , and defined as $\mathbf{h}_{p,e} = (\mathbf{g}_{b,e}^p)^H + \mathbf{g}_{p,e}^H \Theta_p \mathbf{H}$. The corresponding achievable rates of s_c and s_n^p at the E^p are $R_{c,e}^p = \log_2(1 + \gamma_{c,e}^p)$, and $R_{e,n}^p = \log_2(1 + \gamma_{e,n}^p)$, $\forall n \in \mathcal{N}, p \in \{t, r\}$. For the Eves, we aim to design the transmission power such that the information messages are not decodable at the Eves. In order to achieve this goal, the condition $\max_{p \in \{t, r\}} \{R_{c,e}^p\} < R_c$ should be satisfied for the common signal.

We emphasize that we are assuming a worst-case scenario in terms of security, where the Eve knows its CSI and all precoders. Thus, the achievable secrecy rate between the BS-RIS and each legitimate user is given by:

$$\begin{aligned} R_{sec,n}^{tot} &\triangleq R_{sec,c} + R_{sec,n}, \quad \forall n \in \mathcal{N} \\ R_{sec,c} &\triangleq \alpha_n \left[R_c - \max_{p \in \{t, r\}} \{R_{c,e}^p\} \right]^+, \\ R_{sec,n} &\triangleq \left[R_n^p - \max_{p \in \{t, r\}} \{R_{e,n}^p\} \right]^+, \quad \forall n \in \mathcal{N} \end{aligned} \quad (11)$$

where we define the operation $[x]^+ \triangleq \max(0, x)$.

III. PROPOSED SSR MAXIMIZATION

A. Problem Formulation

Our objective is to maximize the SSR of all users with proportional rate constraints. Mathematically, the SSR maximization problem can be posed as follows:

$$\max_{\mathbf{P}, \mathbf{u}_p, \boldsymbol{\alpha}} \left(\min_n \{R_{sec,n}^{tot}\} \right), \quad (12a)$$

$$\text{s.t. } 0 \leq \alpha_n \leq 1, \quad \forall n \in \mathcal{N}, \quad (12b)$$

$$\sum_{n \in \mathcal{N}} \alpha_n = 1, \quad (12c)$$

$$R_c \leq R_{c,n}^p, \quad \forall n \in \mathcal{N}, p \in \{t, r\}, \quad (12d)$$

$$\alpha_n R_c \geq r_c, \quad \forall n \in \mathcal{N} \quad (12e)$$

$$\|\mathbf{P}\|_F^2 \leq P_t, \quad (12f)$$

$$\beta_m^p \in \mathbb{R}_\beta, \quad \theta_m^p \in \mathbb{R}_\theta, \quad \forall m \in \mathbb{M}, \quad \forall p \in \{t, r\}, \quad (12g)$$

where r_c is a predefined threshold, $\boldsymbol{\alpha} \triangleq [\alpha_1, \alpha_2, \dots, \alpha_N]^T$. The constraint (12e) is specifically included to address the rate requirement for the common message. Problem (12) poses challenges due to its nonconvex objective and constraints, complicating the identification of an optimal solution. We address this by applying SCA, which breaks down the problem into simpler, convex subproblems. At each iteration, complex constraints are replaced with convex approximations for easier resolution.

B. SCA-based Solution for Precoder Optimization

Initiating with the STAR-RIS beamforming vector \mathbf{u}_p , our objective is to refine the precoder vectors \mathbf{P} . Utilizing SCA, we first transform and linearize variables to mitigate non-convexity. We then iteratively linearize non-convex terms via

their first-order Taylor expansions, crafting convex approximations for streamlined analysis and optimization.

1) Non-Convex Objective Function (12a)

First, we remove the inner minimization of the max-min problem (12). We introduce an auxiliary variable r_{sec} and reframe both the objective and constraints of (12) accordingly.

$$\max_{\mathbf{P}, \boldsymbol{\alpha}} r_{sec} \quad (13a)$$

$$\text{s.t. } \alpha_n \left[R_c - \max_{p \in \{t, r\}} \{R_{c,e}^p\} \right]^+ +$$

$$\left[R_n^p - \max_{p \in \{t, r\}} \{R_{e,n}^p\} \right]^+ \geq r_{sec}, \quad \forall n \in \mathcal{N}, \quad (13b)$$

$$(12b) - (12f) \quad (13c)$$

r_{sec} acts as a minimum limit for $\min_k R_{sec,n}^{tot}$, and by maximizing it, we enhance the lower side of constraints (13b), ensuring the constraint is met at the best solution. To reach (13), we replaced $R_{sec,c}$ and $R_{sec,n}$ in (13b) with their definitions from (11). The presence of the operator $[\cdot]^+$ makes constraint (13b) nonconvex. To simplify, we introduce two new constraints, (14e) and (14f), to bypass this operator. We also introduce new auxiliary variables $\boldsymbol{\alpha}_c \triangleq [\alpha_{c,1}, \alpha_{c,2}, \dots, \alpha_{c,J}]^T$ and $\boldsymbol{\alpha}_p \triangleq [\alpha_{p,1}, \alpha_{p,2}, \dots, \alpha_{p,K}]^T$, where $\boldsymbol{\alpha}_{p,k} \triangleq [\alpha_{p,k,1}, \alpha_{p,k,2}, \dots, \alpha_{p,k,J}]^T$, $\forall k \in \mathcal{K}$ to aid in making (13) convex. This approach transforms (13) accordingly.

$$\max_{\mathbf{P}, \boldsymbol{\alpha}, \boldsymbol{\alpha}_c, \boldsymbol{\alpha}_p} r_{sec} \quad (14a)$$

$$\text{s.t. } \alpha_n (R_c - \alpha_{c,e}) + \gamma_n - \alpha_{n,e} \geq r_{sec}, \quad \forall n \in \mathcal{N}, \quad (14b)$$

$$R_{c,e}^p \leq \alpha_{c,e}, \quad \forall p \in \{t, r\}, \quad (14c)$$

$$R_{e,n}^p \leq \alpha_{n,e}, \quad \forall n \in \mathcal{N}, p \in \{t, r\}, \quad (14d)$$

$$R_c \geq \alpha_{c,e}, \quad (14e)$$

$$\gamma_n \geq \alpha_{n,e}, \quad \forall n \in \mathcal{N}, \quad (14f)$$

$$\gamma_n \leq R_n^p, \quad \forall n \in \mathcal{N}, p \in \{t, r\} \quad (14g)$$

$$(12b) - (12f) \quad (14h)$$

The discussion indicates that γ_n serves as a lower-bound for R_n^p , whereas $\alpha_{c,e}$ and $\alpha_{n,e}$ provide upper-bounds for $\max_{p \in \{t, r\}} R_{c,e}^p$ and $\max_{p \in \{t, r\}} R_{e,n}^p$, respectively. By increasing the lower-bound and decreasing the upper-bounds, we improve the left-hand side of the constraints, making constraints (14b)-(14g) active in the optimal solution.

Despite linearizing, the constraints (14b)-(14d), and (14g) remain non-convex due to the nature of $R_{c,e}^p$, $R_{e,n}^p$, and R_n^p . To address this, we approximate these constraints with an inner convex subset. Specifically, we use the first-order Taylor expansion for (14b), resulting in $\Theta^{[i]}(\alpha_n, R_c) - \Theta^{[i]}(\alpha_n, \alpha_{c,e}) + \gamma_n - \alpha_{n,e} \geq r_{sec}$, with the definitions $\Theta^{[i]}(x, y) \triangleq \frac{1}{2}(x^{[i]} + y^{[i]})(x + y) - \frac{1}{4}(x^{[i]} + y^{[i]})^2 - \frac{1}{4}(x - y)^2$, and $\Theta^{[i]}(x, y) \triangleq \frac{1}{4}(x + y)^2 + \frac{1}{4}(x^{[i]} - y^{[i]})^2 - \frac{1}{2}(x^{[i]} - y^{[i]})(x - y)$, for linearly approximating the product terms.

The constraints in (14c), (14d), and (14g) are still non-convex. To handle the non-convexity of these constraints we build a suitable inner convex subset to approximate

the nonconvex feasible solution set. In particular, we first define a set of new auxiliary variables $\pi_{c,j,j',k} \triangleq [\rho_{c,j}, \rho_{k,j}, \rho_k, a_{j,k}, b_{j,j'}, x_{c,j}, x_{k,j}, v_j], \forall k \in \mathcal{K}, \{j, j'\} \in \mathcal{J}$ and exploit the following Propositions.

Proposition 1. An affine approximation of constraint (14c), $\forall p \in \{t, r\}$ is given by:

$$\begin{cases} \text{(I)} : 1 + \rho_{c,e}^p - \Gamma^{[i]}(\alpha_{c,e}) \leq 0, \\ \text{(II)} : \frac{(x_{c,e}^p)^2}{\sum_{n \in \mathcal{N}} a_{e,n}^p + 1} \leq \rho_{c,e}^p, \\ \text{(III)} : |\mathbf{h}_{p,e} \mathbf{p}_c| \leq x_{c,e}^p, \\ \text{(IV)} : \Psi^{[i]}(\mathbf{p}_n, 1; \mathbf{h}_{p,e}) \geq a_{e,n}^p, \end{cases} \quad (15)$$

where $\Gamma^{[i]}(x) \triangleq 2x^{[i]} [1 + \ln(2)(x - x^{[i]})]$, and $\Psi^{[i]}(\mathbf{u}, x; \mathbf{h}) \triangleq \frac{2\Re\{\mathbf{u}^{[i]H} \mathbf{h} \mathbf{h}^H \mathbf{u}\}}{x^{[i]}} - \frac{|\mathbf{h}^H \mathbf{u}^{[i]}|^2}{(x^{[i]})^2}$

Proof. Please refer to [4]. ■

Proposition 2. An affine approximation of constraint (14d), $\forall n \in \mathcal{N}, p \in \{t, r\}$ is given by:

$$\begin{cases} \text{(I)} : 1 + \rho_{n,e}^p - \Gamma^{[i]}(\alpha_{n,e}) \leq 0, \\ \text{(II)} : \frac{(x_{n,e}^p)^2}{v_e^p + \sum_{n' \in \mathcal{N}, n' \neq n} a_{e,n'}^p + 1} \leq \rho_{n,e}^p, \\ \text{(III)} : |\mathbf{h}_{p,e} \mathbf{p}_n| \leq x_{n,e}^p, \\ \text{(IV)} : \Psi^{[i]}(\mathbf{p}_c, 1; \mathbf{h}_{p,e}) \geq v_e^p, \end{cases} \quad (16)$$

Proof. This Proposition can be proved following the same approach as presented in [4]. ■

Proposition 3. An affine approximation of constraint (14g), $\forall n \in \mathcal{N}, p \in \{t, r\}$ is given by:

$$\begin{cases} \text{(I)} : 1 + \rho_n - 2^{\gamma_n} \geq 0, \\ \text{(II)} : \sum_{n' \in \mathcal{N}, n' \neq n} |\mathbf{h}_{p,n} \mathbf{p}_{n'}|^2 - \Psi^{[i]}(\mathbf{p}_n, \rho_n; \mathbf{h}_{p,n}) + 1 \leq 0, \end{cases} \quad (17)$$

Proof. See [4]. ■

2) Non-convex constraint (12d)

To handle the nonconvexity of (12d), we first introduce the new auxiliary variables $\rho_{c,k} \forall k \in \mathcal{K}$ and resort to Proposition 4, as follows:

Proposition 4. An affine approximation of constraint (12d), $\forall n \in \mathcal{N}, p \in \{t, r\}$ is given by:

$$\begin{cases} \text{(I)} : 1 + \rho_{c,n} - 2^{R_c} \geq 0, \\ \text{(II)} : \sum_{n' \in \mathcal{N}} |\mathbf{h}_{p,n} \mathbf{p}_{n'}|^2 - \Psi^{[i]}(\mathbf{p}_c, \rho_{c,n}; \mathbf{h}_{p,n}) + 1 \leq 0. \end{cases} \quad (18)$$

Proof. This Proposition is proved by following the same approach presented in [4]. ■

3) Non-convex constraint (12e)

To handle the nonconvexity of (12e), we utilize Proposition 5, as follows:

Proposition 5. An affine approximation of constraint (12e), $\forall n \in \mathcal{N}$ is given by:

$$\Theta^{[i]}(\alpha_n, R_c) \geq r_c. \quad (19)$$

Proof. See [4]. ■

With these approximations, we detail the SCA-based methodology in Algorithm 1, where we solve the ensuing convex optimization problem:

$$\begin{aligned} & \max_{\mathbf{x}} r_{sec} \\ & \text{s.t. (14b), (14e), (14f), (12b), (12c),} \\ & (15) - (19), \bar{\omega} \geq 0 \end{aligned} \quad (20)$$

where $\bar{\omega} \triangleq [\gamma_n, \alpha_c, \alpha_p, \pi_{c,n}, \rho_{c,n}], \forall n \in \mathcal{N}, p \in \{t, r\}$, and $\mathbf{x} \triangleq [\mathbf{P}, \alpha, \bar{\omega}]$. Given feasible starting points for (20), the solutions and feasible set determined by its constraints are assured to fit within the original set outlined in (12). This process is repeated until it meets the stopping condition or reaches the set iteration limit.

Algorithm 1 SCA-based Algorithm for Precoder Optimization

- 1: **Input:** Set the threshold value for accuracy (δ_I) and the maximum number of iterations (N_{max}).
 - 2: **Initialization:** Initialize $\mathbf{x}^{[i]}$ with a feasible initialization point and set $i = 0$.
 - 3: **while** $|r_{sec}^{[m+1]} - r_{sec}^{[i]}| \geq \delta_I$ or $i \leq N_{max}$ **do** **(I)-(III)**
 - 4: **I:** Find $\mathbf{x}^{[i+1]}$ by solving (20).
 - 5: **II:** Update the slack variables based on $\mathbf{x}^{[i+1]}$.
 - 6: **III:** $i = i + 1$.
 - 7: **end while**
 - 8: **Output:** \mathbf{P}^* .
-

C. SCA-based Solution for Transmission and Reflection Beamforming Optimization

For the next step, for any given precoder vectors \mathbf{p}_c , and \mathbf{p}_n , the optimization problem for the RIS beamforming vector \mathbf{u}_p inspired by (14) is reformulated as

$$\max_{\mathbf{u}_p} r_{sec}, \quad (21a)$$

$$\text{s.t. } \alpha_n(R_c - \alpha_{c,e}) + \gamma_n - \alpha_{n,e} \geq r_{sec}, \forall n \in \mathcal{N}, \quad (21b)$$

$$R_{c,e}^p \leq \alpha_{c,e}, \forall p \in \{t, r\}, \quad (21c)$$

$$R_{e,n}^p \leq \alpha_{n,e}, \forall n \in \mathcal{N}, p \in \{t, r\}, \quad (21d)$$

$$R_c \geq \alpha_{c,e}, \quad (21e)$$

$$\gamma_n \geq \alpha_{n,e}, \forall n \in \mathcal{N}, \quad (21f)$$

$$\gamma_n \leq R_n^p, \forall n \in \mathcal{N}, p \in \{t, r\} \quad (21g)$$

$$\alpha_n R_c \geq r_c, \forall n \in \mathcal{N}, \quad (21h)$$

$$R_c \leq R_{c,n}^p, \forall n \in \mathcal{N}, p \in \{t, r\}, \quad (21i)$$

$$\beta_m^p, \theta_m^p \in \mathbb{R}_{\beta, \theta}, \forall m \in \mathbb{M}, \forall p \in \{t, r\}, \quad (21j)$$

Before solving this problem, we first transform (21) into a more tractable form. Given the precoders \mathbf{p}_c , and \mathbf{p}_n , let $\mathbf{G}_{\mathbf{p}, \mathbf{q}} = \begin{bmatrix} \text{diag}(\mathbf{g}_{p,q}^H) \mathbf{H} \\ (\mathbf{g}_{b,q}^p)^H \end{bmatrix}$, and $\mathbf{v}_p = [\mathbf{u}_p \ 1]^H$, where $p \in \{t, r\}, q \in \{\mathcal{K}, \mathcal{J}, e\}$. Moreover, we define $\bar{\mathbf{h}}_{p,q,c} \triangleq \mathbf{G}_{\mathbf{p}, \mathbf{q}} \mathbf{p}_c$, and $\bar{\mathbf{h}}_{p,q,n} \triangleq \mathbf{G}_{\mathbf{p}, \mathbf{q}} \mathbf{p}_n$. Then, for all $n \in \mathcal{N}, p \in \{t, r\}$, and

$q \in \{\mathcal{K}, \mathcal{J}, e\}$ we have:

$$|\mathbf{h}_{p,q}\mathbf{p}_c|^2 = |\mathbf{v}_p^H \bar{\mathbf{h}}_{p,q,c}|^2 = \text{Tr}(\mathbf{V}_p \bar{\mathbf{H}}_{p,q,c}), \quad (22)$$

$$|\mathbf{h}_{p,q}\mathbf{p}_n|^2 = |\mathbf{v}_p^H \bar{\mathbf{h}}_{p,q,n}|^2 = \text{Tr}(\mathbf{V}_p \bar{\mathbf{H}}_{p,q,n}), \quad (23)$$

where $\mathbf{V}_p = \mathbf{v}_p \mathbf{v}_p^H$, $\mathbf{V}_p \succeq 0$, $\text{rank}(\mathbf{V}_p) = 1$, and $[\mathbf{V}_p]_{m,m} = \beta_m^p$, $p \in \{t, r\}$. Moreover, $\bar{\mathbf{H}}_{p,q,c} = \bar{\mathbf{h}}_{p,q,c} \bar{\mathbf{h}}_{p,q,c}^H$, and $\bar{\mathbf{H}}_{p,q,n} = \bar{\mathbf{h}}_{p,q,n} \bar{\mathbf{h}}_{p,q,n}^H$. Before solving problem (21), we also introduce a slack variable set $\{A_{p,q,c}, B_{p,q,c}, A_{p,q,n}, B_{p,q,n} | n \in \mathcal{N}, p \in \{t, r\}, q \in \{\mathcal{K}, \mathcal{J}, e\}\}$ defined as

$$\frac{1}{A_{p,q,c}} = \text{Tr}(\mathbf{V}_p \bar{\mathbf{H}}_{p,q,c}), \quad (24)$$

$$B_{p,q,c} = \sum_{n \in \mathcal{N}} \text{Tr}(\mathbf{V}_p \bar{\mathbf{H}}_{p,q,n}) + 1, \quad (25)$$

$$\frac{1}{A_{p,q,n}} = \text{Tr}(\mathbf{V}_p \bar{\mathbf{H}}_{p,q,n}), \quad (26)$$

$$B_{p,n} = \sum_{n' \in \mathcal{N}, n' \neq n} \text{Tr}(\mathbf{V}_p \bar{\mathbf{H}}_{p,n,n'}) + 1, \quad (27)$$

$$B_{p,e} = \text{Tr}(\mathbf{V}_p \bar{\mathbf{H}}_{p,e,c}) + \sum_{n' \in \mathcal{N}, n' \neq n} \text{Tr}(\mathbf{V}_p \bar{\mathbf{H}}_{p,e,n'}) + 1, \quad (28)$$

Substituting (24) and (25) into (5), (9) and (26)-(28) into (6) and (10), the achievable data rates for the common and private streams of users, respectively, can be rewritten as

$$R_{c,q}^p = \log_2 \left(1 + \frac{1}{A_{p,q,c} B_{p,q,c}} \right), \quad (29)$$

$$R_q^p = \log_2 \left(1 + \frac{1}{A_{p,q,n} B_{p,q}} \right), \quad (30)$$

where $n \in \mathcal{N}$, $p \in \{t, r\}$, $q \in \{\mathcal{K}, \mathcal{J}, e\}$. The surrogate equations (29) and (30) to be used in place of (21g) and (21i) are still non-convex. However, $\log_2 \left(1 + \frac{1}{xy} \right)$ is a joint convex function with respect to x and y , so using a first-order Taylor expansion we approximate the right-hand terms of (29) and (30) by the following lower bounds:

$$\log_2 \left(1 + \frac{1}{A_{p,n,c} B_{p,n,c}} \right) \geq \tilde{R}_{c,n}^p = \log_2 \left(1 + \frac{1}{A_{p,n,c}^{[l]} B_{p,n,c}^{[l]}} \right) - \frac{\log_2(e)(A_{p,n,c} - A_{p,n,c}^{[l]})}{A_{p,n,c}^{[l]} + (A_{p,n,c}^{[l]})^2 B_{p,n,c}^{[l]}} - \frac{\log_2(e)(B_{p,n,c} - B_{p,n,c}^{[l]})}{B_{p,n,c}^{[l]} + (B_{p,n,c}^{[l]})^2 A_{p,n,c}^{[l]}} \quad (31)$$

$$\log_2 \left(1 + \frac{1}{A_{p,n,n} B_{p,n}} \right) \geq \tilde{R}_n^p = \log_2 \left(1 + \frac{1}{A_{p,n,n}^{[l]} B_{p,n}^{[l]}} \right) - \frac{\log_2(e)(A_{p,n,n} - A_{p,n,n}^{[l]})}{A_{p,n,n}^{[l]} + (A_{p,n,n}^{[l]})^2 B_{p,n}^{[l]}} - \frac{\log_2(e)(B_{p,n} - B_{p,n}^{[l]})}{B_{p,n}^{[l]} + (B_{p,n}^{[l]})^2 A_{p,n,n}^{[l]}} \quad (32)$$

where $A_{p,n,c}^{[l]}$, $B_{p,n,c}^{[l]}$, $A_{p,n,n}^{[l]}$, and $B_{p,n}^{[l]}$ represent the values of $A_{p,n,c}$, $B_{p,n,c}$, $A_{p,n,n}$, and $B_{p,n}$ in the l -th iteration, respectively. Thus, the transmission and reflection beamforming optimization problem in (21) with fixed precoders can be reformulated as

$$\max_{\mathbf{u}_p} r_{sec}, \quad (33a)$$

$$\text{s.t.} \quad \frac{1}{A_{p,q,c}} \leq \text{Tr}(\mathbf{V}_p \bar{\mathbf{H}}_{p,q,c}), \quad (33b)$$

$$B_{p,q,c} \geq \sum_{n \in \mathcal{N}} \text{Tr}(\mathbf{V}_p \bar{\mathbf{H}}_{p,q,n}) + 1, \quad (33c)$$

$$\frac{1}{A_{p,q,n}} \leq \text{Tr}(\mathbf{V}_p \bar{\mathbf{H}}_{p,q,n}), \quad (33d)$$

$$B_{p,n} \geq \sum_{n' \in \mathcal{N}, n' \neq n} \text{Tr}(\mathbf{V}_p \bar{\mathbf{H}}_{p,n,n'}) + 1, \quad (33e)$$

$$B_{p,e} \geq \text{Tr}(\mathbf{V}_p \bar{\mathbf{H}}_{p,e,c}) + \sum_{n' \in \mathcal{N}, n' \neq n} \text{Tr}(\mathbf{V}_p \bar{\mathbf{H}}_{p,e,n'}) + 1, \quad (33f)$$

$$\alpha_{c,e} \geq \log_2 \left(1 + \frac{1}{A_{p,e,c} B_{p,e,c}} \right), \quad (33g)$$

$$\alpha_{n,e} \geq \log_2 \left(1 + \frac{1}{A_{p,e,n} B_{p,e}} \right), \quad (33h)$$

$$R_c \leq \tilde{R}_{c,n}^p, \quad (33i)$$

$$\gamma_n \leq \tilde{R}_n^p, \quad (33j)$$

$$\beta_m^t + \beta_m^r = 1, \quad (33k)$$

$$[\mathbf{V}_p]_{m,m} = \beta_m^p, \quad (33l)$$

$$\mathbf{V}_p \succeq 0, \quad (33m)$$

$$\text{rank}(\mathbf{V}_p) = 1, \quad (33n)$$

$$(21b), (21e), (21f), (21h) \quad (33o)$$

where $p \in \{t, r\}$, $n \in \mathcal{N}$, $q \in \{\mathcal{K}, \mathcal{J}, e\}$, and $m \in \mathbb{M}$. As in [9], [10], the non-convex rank-one constraint (33n) can be replaced by the following relaxed convex constraint:

$$e_{max}^H(\mathbf{V}_p^{[l]}) \mathbf{V}_p e_{max}(\mathbf{V}_p^{[l]}) \geq \epsilon^{[l]} \text{Tr}(\mathbf{V}_p), \quad (34)$$

where $e_{max}(\mathbf{V}_p^{[l]})$ is the eigenvector corresponding to the maximum eigenvalue of $\mathbf{V}_p^{[l]}$ and $\epsilon^{[l]}$ is a relaxation parameter in the l -th iteration. Specifically, $\epsilon^{[l]} = 0$ indicates that the rank-one constraint is dropped, while $\epsilon^{[l]} = 1$ means it is retained. Therefore, we can increase $\epsilon^{[l]}$ from 0 to 1 with each iteration to gradually approach a rank-one solution. Thus, solving problem (33) is transformed to solving the following relaxed problem:

$$\max_{\mathbf{u}_p} r_{sec}, \quad (35a)$$

$$\text{s.t.} \quad (21b), (21e), (21f), (21h), (33b) - (33m), (34) \quad (35b)$$

Problem (35) is a standard convex SDP, which can be solved efficiently by numerical solvers such as the SDP tool in CVX [11]. Building on the above discussions, we outline a two-step iterative algorithm to address the original problem (12). This method involves alternating optimization of the precoders with the optimization of the passive beamforming vectors.

IV. SIMULATION RESULTS

This section presents numerical results for our STAR-RIS-RSMA system simulation. The BS is placed at (0, 0, 20) meters, and the RIS at (0, 30, 20). We consider $K = 3$ and $J = 3$ users positioned on each side of the RIS. Path loss for user n , $\text{PL}_n = d_n^{-\eta_n}$, incorporates distance d_n to the RIS and path loss exponent $-\eta_n$, based on the model of [12]. In

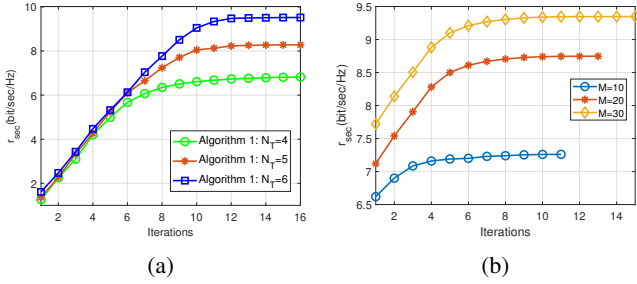


Fig. 2: (a) Convergence of Algorithm 1 for different values of N_T , when $P_t = 25\text{dBm}$ and $M = 10$ and (b) convergence of (35) for different values of M , when $N_T = 4$.

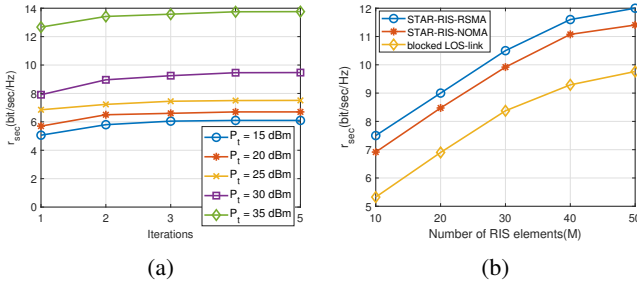


Fig. 3: (a) Convergence of the whole algorithm against iteration number for various transmit powers, with $N_T = 4$ and $M = 10$, and (b) Comparison of the proposed method, NOMA, and RSMA under direct link blockage [7].

particular, the model assumes

$$\eta_n \triangleq \frac{\mathcal{L}_n - \mathcal{N}_n}{1 + \lambda_1 e^{\lambda_2(\phi_n - \lambda_1)}} + \mathcal{N}_n, \quad (36)$$

The exponent η_n blends line-of-sight (LoS) and non-LoS components, affected by the elevation angle and environment factors, with LoS and NLoS exponents set at $\mathcal{L} = 2$ and $\mathcal{N} = 3.5$. Results average over 100 channel realizations, with algorithmic parameters $N_{max} = M_{max} = 30$ and threshold $\delta_I = 10^{-2}$. The additive noise at the receiver side is considered to have a normalized power of 0 dBm, the minimum required rate of common stream transmissions is $r_c = 1$.

Fig. 2a examines the impact of varying N_T on Algorithm 1's efficacy, noting that additional transmit antennas boost degrees of freedom and thus r_{sec} . Fig. 2b explores the convergence of problem (35), revealing that higher M values extend the iterations needed for convergence due to the optimization of more transmission and reflection coefficients, while also significantly enhancing the achievable secrecy rate.

Fig. 3a demonstrates the rapid convergence of the whole two-step Algorithm within a few iterations, highlighting the algorithm's efficacy. Additionally, it shows that r_{sec} notably increases in scenarios with high transmit power. Fig. 3b compares the proposed method with NOMA and RSMA in situations of direct link blockage, clearly demonstrating the superior performance of our method.

V. CONCLUSIONS

In this paper, we introduced a STAR-RIS-RSMA technique to boost secure communication in MISO networks, aiming to maximize the sum secrecy rate of legitimate users within transmit power constraints. This involved co-optimizing precoder vectors and RIS transmission/reflection coefficients. Given the non-convex nature and complex variable interdependencies of the problem, we devised a suboptimal two-step iterative algorithm for alternately optimizing precoders and RIS coefficients. Simulation results confirm the efficacy of our approach, showing that increased BS antenna count enhances system performance. Additionally, higher M values lead to improved rates, with our method demonstrating robust convergence and significant secrecy rate achievements. Ultimately, our approach demonstrated superior performance with respect to NOMA.

ACKNOWLEDGMENT

This research is supported by the HORIZON JU-SNS-2022-STREAM-B-01-03 6G-SHINE project (Grant Agreement No.101095738).

REFERENCES

- [1] M. Di Renzo, et al., "Smart radio environments empowered by AI reconfigurable meta-surfaces: An idea whose time has come," *EURASIP J. Wireless Commun.*, vol. 129, May 2019.
- [2] X. Mu, Y. Liu, L. Guo, J. Lin, and R. Schober, "Simultaneously transmitting and reflecting (STAR) RIS aided wireless communications," *IEEE Trans. Commun.*, vol. 21, no. 5, pp. 3083-3098, May 2022
- [3] G. Berardinelli et al., "Extreme Communication in 6G: Vision and Challenges for 'in-X' Subnetworks," *IEEE Open Journal of the Communications Society*, vol. 2, pp. 2516-2535, 2021.
- [4] H. Bastami, M. Letafati, M. Moradikia, A. Abdelhadi, H. Behroozi and L. Hanzo, "On the Physical Layer Security of the Cooperative Rate-Splitting-Aided Downlink in UAV Networks," *IEEE Transactions on Information Forensics and Security*, vol. 16, pp. 5018-5033, 2021.
- [5] Y. Mao, B. Clerckx, and V. O. Li, "Rate-splitting multiple access for downlink communication systems: bridging, generalizing, and outperforming SDMA and NOMA," *EURASIP J. Wireless Commun. Netw.*, vol. 1, pp. 1-54, 2018.
- [6] C. Meng, K. Xiong, W. Chen, B. Gao, P. Fan and K. B. Letaief, "Sum-Rate Maximization in STAR-RIS-Assisted RSMA Networks: A PPO-Based Algorithm," *IEEE Internet of Things Journal*, vol. 11, no. 4, pp. 5667-5680, 15 Feb.15, 2024.
- [7] H. R. Hashempour, H. Bastami, M. Moradikia, S. A. Zekavat, H. Behroozi, and A. L. Swindlehurst, "Secure SWIPT in STAR-RIS aided downlink MISO rate-splitting multiple access networks," arXiv preprint arXiv:2211.09081, 2022.
- [8] H. Joudeh and B. Clerckx, "Rate-splitting for max-min fair multigroup multicast beamforming in overloaded systems," *IEEE Transactions on Wireless Communications*, vol. 16, no. 11, pp. 7276-7289, Nov 2017.
- [9] X. Mu, Y. Liu, L. Guo, J. Lin, and N. Al-Dhahir, "Exploiting intelligent reflecting surfaces in NOMA networks: Joint beamforming optimization," *IEEE Trans. Wireless Commun.*, vol. 19, no. 10, pp. 6884-6898, Oct. 2020.
- [10] X. Mu, Y. Liu, L. Guo, J. Lin, and R. Schober, "Joint deployment and multiple access design for intelligent reflecting surface assisted networks," *IEEE Trans. Wireless Commun.*, vol. 20, no. 10, pp. 6648-6664, Oct. 2021.
- [11] M. Grant and S. Boyd, "CVX: Matlab software for disciplined convex programming, version 2.1," <http://cvxr.com/cvx>, Mar. 2014.
- [12] A. Omri and M. O. Hasna, "Physical layer security analysis of UAV based communication networks," in *Proc. IEEE 88th Vehicular Technology Conference (VTC-Fall)*, Chicago, IL, USA, Aug. 2018.